Journal of Thermal Analysis, Vol. 50 (1997) 569-586

THERMAL LATENT COORDINATION COMPOUNDS*
II. The thermal degradation of imidazole and pyrazole adducts of metal(II) picolinate and quinaldinate

M. Döring, J. Wuckelt, W. Ludwig and H. Görls

Institute of Inorganic and Analytical Chemistry, University of Jena, A.-Bebel Strasse 2
D-07743 Jena, Germany

(Received September 19, 1996)

Abstract

Complexes of the type $M(Pa)_2(HAz)_2$ and $M(QA)_2(HAz)_2$ (*M*=cobalt(II) and nickel(II); HPa=picolinic acid, HQa=quinaldic acid; HAz=azoles like imidazole (HIm), pyrazole (HPz), benzimidazole (HBzIm) etc.) show a similar thermal behaviour. In the first step of decomposition the corresponding azolinium picolinates or quinaldinates (H_2AzPa, H_2AzQa) are split off with formation of polymeric mixed ligand complexes M(Pa)(Az) or M(Qa)(Az). X-ray analysis of $Co(Qa)_2(HBzIm)_2$ XIIIa illustrates a proton transfer and a subsequent thermal removal of benzimidazolinium quinaldinate ($H_2BzImQa$): Hydrogen bridges from pyrrole nitrogen of the benzimidazole to the non-coordinated oxygen of the quinaldinate predetermine the thermal initiated proton transfer. The high volatility of the heterocyclic acids and the nitrogen coordination are responsible for the formation of the mixed ligand complex Co(Qa)(BzIm) XIVa.

Exceptions are the complexes $M(Pa)_2(HPz)_2$ XIa-b and $M(Qa)_2(HIm)_2$ XVIIa-b. Pyrazole is eliminated from the complexes XIa-b with formation of the solvent-free inner complex $M(Pa)_2$ XIIa-b. From compounds XVIIIa-b quinaldic acid or their decomposition products are split off and a high temperature modification of $M(Im)_2$ XVIIIa-b is formed at elevated temperature. XVIIIa-b are decomposed to the cyanides $M(CN)_2$ similarly to the thermal behaviour of Cu(Im).

In the first step the thermal degradation of imidazole and pyrazole adducts of copper(II) picolinates and quinaldinates is characterized by the elimination of azoles. The reason for this thermal behaviour is the weaker coordination of the azole heterocycles in copper chelate compounds.

Keywords: crystal structure, metal(II) picolinate and quinaldinate, thermal degradation of imidazole and pyrazole complexes

Introduction

Several metal carboxylates containing imidazoles or pyrazoles have been studied as model substrances for biocatalysts [1]. For example, manganese com-

* For Part I see Ref. [8].

0368–4466/97/ $ 5.00

John Wiley & Sons Limited
Chichester

plexes of picolinic acid (HPa) have been synthesized as biologically interesting molecules to describe manganese catalases in photosystem II [2]. Picolinate anion (Pa) always acts as a bidentate chelating ligand. X-ray structure determinations of the isostructural octahedral aqua adducts $M(Pa)_2(H_2O)_2 \cdot 2H_2O$ Ia-b (*M*=cobalt(II), nickel(II)) identify the chelate effect of the picolinate ion, in which the pyridine nitrogen and one of the carboxyl oxygens act as sticking atoms [3, 4]. Chains of octahedrons are built up in the complexes I by intermolecular hydrogen bridges between the coordinated water and the coordinated oxygen atoms of the neighbouring carboxylate group. In addition, these chains are linked together by intermolecular O–H···O–H···O-hydrogen bridges, as shown in Fig. 1.

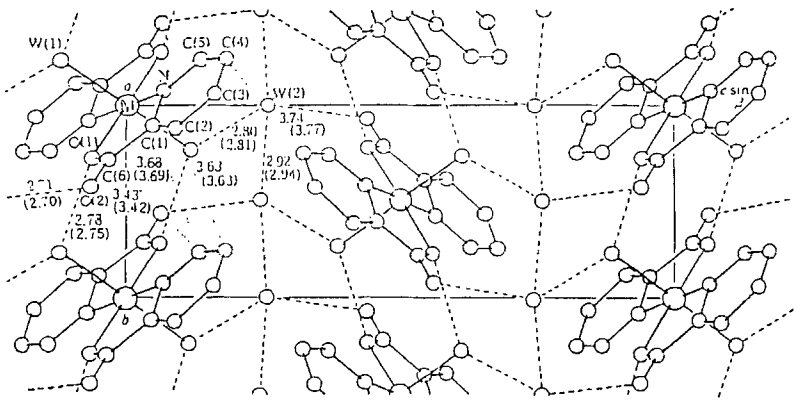

Fig. 1 Section of $Ni(Pa)_2(H_2O) \cdot 2H_2O$ Ib to illustrate the system of intermolecular hydrogen bridges in accordance with Takenaka *et al.* [4b]

Chains of octahedrons are also present in the copper complex $Cu(Pa)_2 \cdot 2H_2O$ Ic. However, they are linked by bridging of the carboxylate groups. Consequently, the typical (4+2)-coordination for copper(II) is obtained. Again, the chains of octahedrons are bonded together by the water molecules. However, in this case both water molecules are necessary to couple the chains [5].

In a similar way, the complex formation reaction of metal(II) picolinates and quinaldinates occurs with imidazoles, benzimidazoles, and pyrazoles forming the bis-adducts $M(Pa)_2(HIm)_2$, $M(Qa)_2(HPz)_2$ etc. Additional water or solvent molecules can be fixed in the second coordination sphere, as found in dihydrates of the type $M(Pa)_2(HIm)_2 \cdot 2H_2O$ or $M(Pa)_2(HPz)_2 \cdot 2H_2O$.

Thermal investigations of the imidazole and pyrazole complexes are based on the ability of such complexes to work as thermal latent epoxy curing agents. While remaining stable at ambient temperature, the azole-metal complexes dissociate at elevated temperature. Henceforth, the released azoles catalyze the homopolymerization of epoxy resins [6].

Thermal degradations of coordination compounds of the type $M(dkt)_2(HIm)_2$ (dkt=1,3-diketonates) are topochemical reactions and the reaction course depends on the crystal structure of these compounds [7]. In addition to this, we were able to show that the thermal behaviour of imidazole- and pyrazole-containing metal acetates differs markedly in respect of the interrelation of kinetic and thermodynamic factors controlled by the variation of the central metal and the nitrogen heterocycle of the chelate adducts. Therefore, either acetic acid or mainly imidazole is eliminated from complexes of the type $M(ac)_2(HIm)_2$ (*M*=Co, Ni, Cu; ac=acetate) under similar conditions. There exists either an acid or a basic thermal latency [8].

We report herein the thermal behaviour of the azole adducts of the corresponding metal(II) picolinates and quinaldinates, and the X-ray crystal structure of $Co(Qa)_2(HBzIm)_2$ XIIIa determined in the course of this study are also described.

Experimental

Synthesis

The complexes VIIa-b, IXa-b, XIa-b, XIIIa-b, XVa-b, and XVIIa-b were prepared according to the following procedure:

To a solution of 1 mmol of cobalt (II) or nickel(II) nitrate hexahydrate in methanol picolinic or quinaldic acid (2 mmol) and 2 mmoles of solid sodium hydroxide were added. The mixture was stirred between 40–50°C until a homogeneous precipitate of the metal(II) picolinate or quinaldinate was separated. After that, 2 mmoles of the azole as a solution in methanol (20 ml) were added. After an additional stirring for two hours, the newly formed precipitate was filtered, repeatedly washed with small portions of cold methanol, and vacuum-dried at room temperature. Melting together copper(II) picolinate $Cu(Pa)_2 \cdot 2H_2O$ or quinaldinate $Cu(Qa)_2 \cdot 2H_2O$ with imidazole or pyrazole, respectively, afforded the copper complexes VIIc, XVc and XVIIc. Subsequent crystallization from dimethylformamide or nitromethane gave pure complexes. Yields and analytical data are listed in Table 1.

Thermal Analysis

The thermobalance designed in our Institute has been described in earlier papers [7a, 9].

X-ray Structure Determination of XIIIa

Crystallographic data pertaining to the structural determination are listed in Table 2.

Table 1 Elemental analysis of complex compounds

Complex compound		Yield/ %	Total molecular formula	Analysis/% calculated/found			
				C	H	N	M
$Co(Pa)_2(Hlm)_2 \cdot 2H_2O$	VIIa	57	$C_{18}H_{20}N_6O_6Co$	45.48	4.25	17.68	12.39
				45.68	3.97	18.08	12.48
$Co(Pa)_2(HBzIm)_2$	IXa	68	$C_{26}H_{20}N_6O_4Co$	54.26	3.74	15.58	10.92
				54.11	3.86	15.45	10.24
$Co(Pa)_2(HPz)_2 \cdot 2H_2O$	XIa	82	$C_{18}H_{20}N_6O_6Co$	45.48	4.25	17.68	12.39
				45.31	4.09	17.67	12.34
$Co(Qa)_2(Hlm)_2$	XVIIa	90	$C_{26}H_{20}N_6O_4Co$	57.88	3.74	15.58	10.92
				57.58	3.88	15.60	11.10
$Co(Qa)_2(HBzIm)_2$	XIIIa	80	$C_{36}H_{24}N_6O_4Co$	63.85	3.78	13.15	9.22
				63.82	4.03	12.97	9.21
$Co(Qa)_2(HPz)_2 \cdot CH_3OH$	XVa	85	$C_{27}H_{24}N_6O_5Co$	56.74	4.20	14.71	10.33
				56.65	4.02	14.85	10.29
$Ni(Pa)_2(Hlm)_2 \cdot 2H_2O$	VIIb	80	$C_{18}H_{20}N_6O_6Ni$	45.50	4.25	17.69	12.35
				45.63	4.00	17.86	12.51
$Ni(Pa)_2(HBzIm)_2$	IXb	74	$C_{26}H_{20}N_6O_4Ni$	57.91	3.75	15.59	10.89
				57.72	3.95	15.61	10.79
$Ni(Pa)_2(HPz)_2 \cdot 2H_2O$	XIb	55	$C_{18}H_{20}N_6O_6Ni$	45.50	4.25	17.69	12.35
				45.37	4.31	17.71	12.44
$Ni(Qa)_2(Hlm)_2$	XVIIb	90	$C_{26}H_{20}N_6O_4Ni$	57.91	3.75	15.59	10.89
				57.82	3.63	14.91	10.95
$Ni(Qa)_2(HBzIm)_2$	XIIIb	93	$C_{34}H_{24}N_6O_4Ni$	63.88	3.78	13.15	9.18
				64.03	4.02	12.92	9.23
$Ni(Qa)_2(HPz)_2 \cdot H_2O$	XVb	90	$C_{26}H_{20}N_6O_5Ni$	56.01	3.95	15.08	10.59
				56.18	4.06	15.07	10.59
$Cu(Pa)_2(Hlm)_2 \cdot 2H_2O$	VIIc	26	$C_{18}H_{20}N_6O_6Cu$	45.04	4.21	17.51	13.24
				45.38	4.26	17.51	13.23
$Cu(Qa)_2(Hlm)_2$	XVIIc	80	$C_{26}H_{20}N_6O_4Cu$	57.39	3.71	15.45	11.68
				57.27	3.94	15.58	11.75
$Cu(Qa)_2(HPz)_2$	XVc	44	$C_{26}H_{20}N_6O_4Cu$	57.39	3.71	15.45	11.68
				57.20	3.79	15.53	11.71

Diffraction data were collected on an Enraf-Nonius CAD 4 diffractometer using graphite monochromated MoK_α radiation (λ=71.069 pm) at room temperature. X-ray intensity of up to Θ_{max}=27°C has been measured by ω–2Θ-scanning. Lorentz and polarisation corrections were applied. No absorption correction was done. The structure was solved by heavy-atom methods (SHELXS-86), which permitted location of the metal atom and most of the non-hydrogen atoms [10]. The coordinates of the remaining non-hydrogen atoms were determined by successive least-squares refinements and difference Fourier maps. The refinements were carried out by full-matrix LSQ-process with anisotropic temperature factors for cobalt. Hydrogen atoms were localized by difference Fourier maps and refined isotropically. The final R-value converged at 0.033 (R_W=0.042).

Table 2 Crystallographic data and data collection parameter for XIIIa

Crystal colour	brown-yellow
Chemical formula	$C_{34}H_{24}N_6O_4Co$
Molecular mass	M_r=639.3 g mol
Crystal size	0.14 mm×0.32 mm×0.32 mm
Crystal system	monoclinic
Space group	$P2_1/n$ (No. 14)
Cell constants	
a	1003.9(2) pm
b	999.3(1) pm
c	1521.9(3) pm
β	108.81(1)°
Cell volume	V=1.4443(1) nm^{-3}
Calculated density	D_C=1.47g cm^{-1}
Molecules per unit cell	Z=2
Absorption coefficient	μ=7.22 cm^{-1} (MoK_α)
Θ_{max}	19°
No. of independent reflexions	3283 (from 3603)
No. of obserced reflexion $I>s\sigma(I)$	2372
No. of parameters	205
R	0.049
R_w	0.057
Final difference fourier	0.68 epm^{-3}

Results and discussion

The picolinates of cobalt, nickel and copper each form with azoles complexes of the type $M(Pa)_2(HAz)_2$. In addition, these complexes form diaqua-adducts (Table 1).

The thermal behaviour of the complexes mentioned can be characterized as follows:

1. Complexes of the type $M(Pa)_2(HAz)_2$ and $M(Qa)_2(HAz)_2$ show a significant thermal stability in comparison with the acetates $M(ac)_2(HAz)_2$ [8] and 1,3-diketonates $M(dkt)_2(HAz)_2$ [7]. Apart from thermal elimination of second sphere coordinated water the thermal decomposition mostly starts at elevated temperatures, frequently above 200°C. This might be due to the low volatilities of free picolinic acid (136°C – sublimation) or quinaldic acid (157°C – decomposition) comparable to acetic acid (*b.p.*: 116°C) or acetylacetone (*b.p.*: 137°C). On the other hand, a coordination core $[MN_4O_2]$ exists in the complexes $M(Pa)_2(HAz)_2$ or $M(Qa)_2(HAz)_2$ while a central unit $[MN_2O_4]$ was found in the corresponding acetates or 1,3-diketonates. Because of the ability of the transition metal(II)ions to nitrogen coordination, an increasing nitrogen environment of the coordination sphere might effect a significant stabilization.

2. The nickel and cobalt complexes $M(Pa)_2(HAz)_2$ and $M(Qa)_2(HAz)_2$ show a similar thermal behaviour. The same thermal degradation steps have been found, only the temperature pattern is different depending on the metal (chapter 3).

3. No oxidation products were found under the described experimental conditions for the cobalt(II) complexes $Co(Pa)_2(HAz)_2$ and $Co(Qa)_2(HAz)_2$. In contrast to this, the complex system Co^{2+}/acen^{2-}2HIm (acen=bis(acetylacetone)ethylendiimine) is oxidized in air to the cobalt(III) cation $[Co(acen)(HIm)_2]^+$ with the same coordination sphere $[CoN_4O_2]$ [11].

In addition to the generally higher thermal stability of the picolinates, the environment richer in nitrogen has a fundamental influence on the released molecules. Earlier investigations of the authors have shown that the same thermal degradation of $M(acac)_2(HIm)_2$ IIa-c and $Niac)_2(HIm)_2$ IVb (Eqs (1, 2)) is based on the large stability of the intermediate coordination polymer $M(Im)_2$ III and also on the comparable crystal structures of IIa-c and IVb [7, 8]: Intermolecular hydrogen bonds between imidazole and acetylacetonate or acetate allows an easy proton transfer from the coordinated heterocycle to the anion. This finally leads to the thermal release of acetylacetone or acetic acid [7, 12].

However, in the first step the cobalt complex IVa releases only one mole of acetic acid forming an acetate and imidazolate bridged tetrahedral species V. The stability of these different bridges seems to be responsible for the following thermal transformation step characterized by the loss of imidazole and imidazolium acetate and formation of the polymeric mixed ligand complex

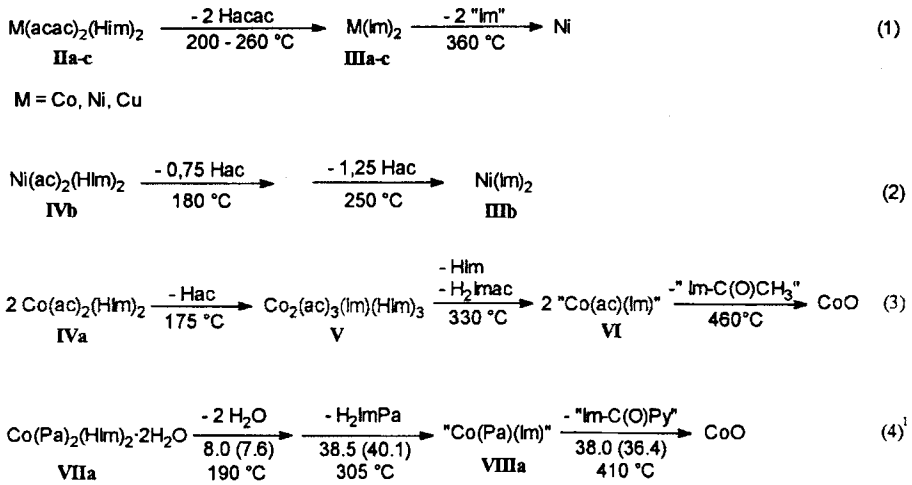

[1]Equations (1) through (14) show the Δm values [%] found without brackets and those obtained by calculation in brackets below the arrows. Temperature data refer to the initial temperature of DTG-curves, i,. e. to the temperature of the completed thermal degradation step.

'Co(ac)(Im)' VI (Eq. 3) [8]. In this context, it is not surprising that IVa and $Co(ac)_2 \cdot 4\ H_2O$ show similar thermal behaviour, but the thermal degradation leads to a hydroxide and acetate bridged intermediate [13].

The thermal formation of polymeric mixed ligand complexes is also favoured in the case of imidazole-containing metal(II) picolinates. Thus, after releasing the water molecules of the second coordination sphere, the complex $Co(Pa_2(HIm)_2 \cdot 2H_2O$ VIIa decomposes in a further step with elimination of imidazolium picolinate (H_2ImPa) to yield the mixed ligand complex Co(Pa)(Im) VIIa (Eq. (4)).

This behaviour was also observed for the benzimidazole adduct $Co(Pa)_2(HBzIm)_2$ IXa (Fig. 2) resulting the coordination polymer Co(Pa)(BzIm) Xa as an intermediate. The corresponding nickel complexes show an analogous thermal behaviour in contrast to the acetate complexes (Eqs (2, 3, 5)). The reason for the similar decomposition patterns of imidazole- and benzimidazole-containing cobalt(II) and nickel(II) picolinates VIIa-b and IXa-b and quinaldinates XIIa-b and XVa-b(see the following section) is the stability of the corresponding mixed ligand intermediates M(Pa)(Az) or M(Qa)(Az). (These complexes contain both imidazolato-bridges and chelating picolinate or quinaldinate in their coordination sphere [$M(N_3O)$].) and the readily volatility of the azolium picolinates are quinaldinates (H_2ImPa, $H_2BzImPa$, $H_2BzImQa$), respectively. The azolium salts sublime undecomposed in the observed high temperature range (Figs 2, 5, 6).

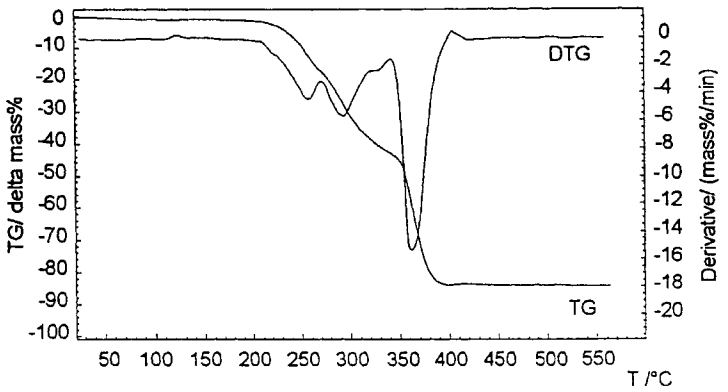

$$Co(Pa)_2(HBzIm)_2 \xrightarrow[43.9\ (44.5)\ 350\ °C]{-\ HBzIm\ -\ HPa} \underset{\textbf{Xa}}{\text{"Co(Pa)(Bzlm)"}} \xrightarrow[40.7\ (41.3)\ 405\ °C]{-\ Bzlm\text{-}C(O)Py} CoO$$

$$\underset{\textbf{IXa}}{Co(Pa)_2(HBzIm)_2}$$

$$Ni(Pa)_2(HBzIm)_2 \xrightarrow[43.9\ (44.9)\ 350\ °C]{-\ HBzIm\ -\ HPa} \underset{\textbf{Xb}}{\text{"Ni(Pa)(Bzlm)"}} \xrightarrow[40.7\ (41.3)\ 405\ °C]{-\ Bzlm\text{-}C(O)Py} NiO \qquad (5)$$

$$\underset{\textbf{IXb}}{Ni(Pa)_2(HBzIm)_2}$$

Fig. 2 Thermal degradation of $Co(Pa)_2(HBzIm)_2$ IXa (TG thermogravimetry, DTG derivative thermogravimetry)

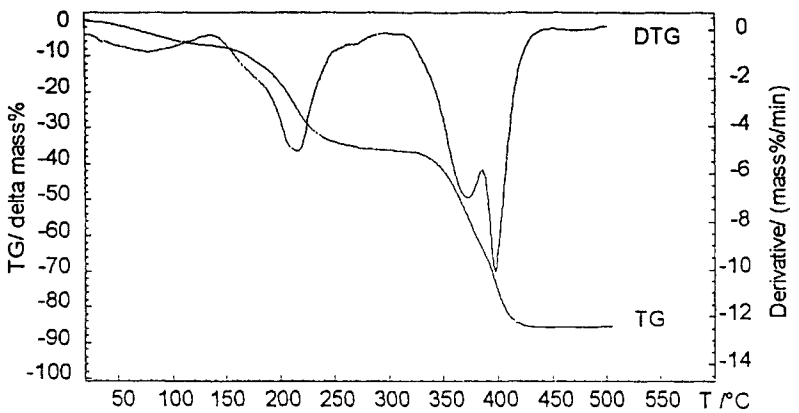

$$Ni(Pa)_2(HPz)_2{\cdot}2H_2O \xrightarrow[7.1\ (7.6)\ 130\ °C]{-\ 2H_2O} \xrightarrow[28.9\ (28.6)\ 300\ °C]{-\ 2\ HPz} \underset{\textbf{XIIb}}{Ni(Pa)_2} \xrightarrow[49.6\ (48.0)\ 450\ °C]{} NiO$$

$$\underset{\textbf{XIb}}{Ni(Pa)_2(HPz)_2{\cdot}2H_2O}$$

$$Co(Pa)_2(HPz)_2{\cdot}2H_2O \xrightarrow[5.4\ (7.6)\ 100\ °C]{-\ 2H_2O} \xrightarrow[14.3\ (14.4)\ 195\ °C]{-\ HPz} \xrightarrow[14.4\ (15.8)\ 325\ °C]{-\ HPz} \underset{\textbf{XIIa}}{Co(Pa)_2} \xrightarrow[46.6\ (48.0)\ 425\ °C]{} CoO \qquad (6)$$

$$\underset{\textbf{XIa}}{Co(Pa)_2(HPz)_2{\cdot}2H_2O}$$

Fig. 3 Thermal degradation of $Ni(Pa)_2(HPz)_2{\cdot}2H_2O$ XIb

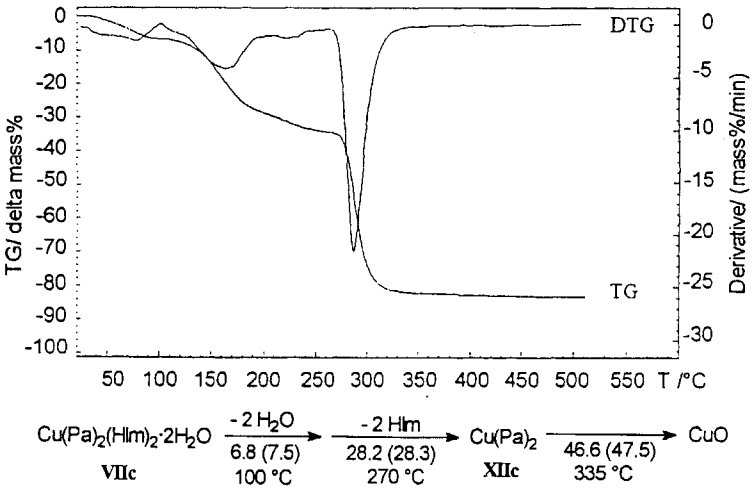

Fig. 4 Thermal degradation of $Cu(Pa)_2(HIm)_2 \cdot 2H_2O$ VIIc

A further explanation of the thermal degradation pattern may be found in the structure of the starting complexes. The dihydrates VIIa-b are supposed to have a structure similar to that of the complexes $M(Pa)_2(H_2O)_2 \cdot 2H_2O$ I (Fig. 1). While the hydrogen bridging system remains unmodified, the apical water molecules are replaced by the imidazoles. The exchange of the water ligands for imidazole and retention of the hydrogen bridges has also been found in the case of ionic complexes [9, 14]. In contrast to the thermolysis of the complexes $Ni(ac)_2(HPz)_4 \cdot H_2O$ [8] and $Co(ba)_2(HIm)_2 \cdot 2CH_3OH$ (ba=benzoylacetonate) [7b] the water of the second coordination sphere of the complexes VIIa-b has no effect on their thermal degradation. In the first step the additional coordinated solvent molecules were always split off. This means that the thermal degradation and the possible proton transfer markedly depends on the molecular structure of the complexes $M(Pa)_2(HAz)_2$ and $M(Qa)_2(HAz)_2$.

Hydrogen bridges between pyrrole nitrogen of the coordinated heterocycle and chelating picolinate or quinaldinate predetermine the proton transfer. A characteristic crystal structure is discussed in section 4. This finally leads to the elimination of azolium picolinate or quinaldinate, respectively (Figs 2, 5, 6).

In the last thermal reaction step the mixed ligand intermediates M(Pa)(Im) VIIIa-b and M(Pa)(BzIm) Xa-b decompose into the metal oxides while formally eliminating N-picolyl imidazoles [Im-C(O)Py or BzIm-C(O)Py] which are immediately transformed into the mentioned imidazolium picolinates (H_2ImPa and H_2BzImPa respectively) by atmospheric humidity [15]. Two peaks or one peak with a shoulder in an elevated temperature range are characteristic of this degradation step (Figs 2, 5, 6). This decomposition pattern is also observed in the case of imidazolato-cobalt(II) acetate [8].

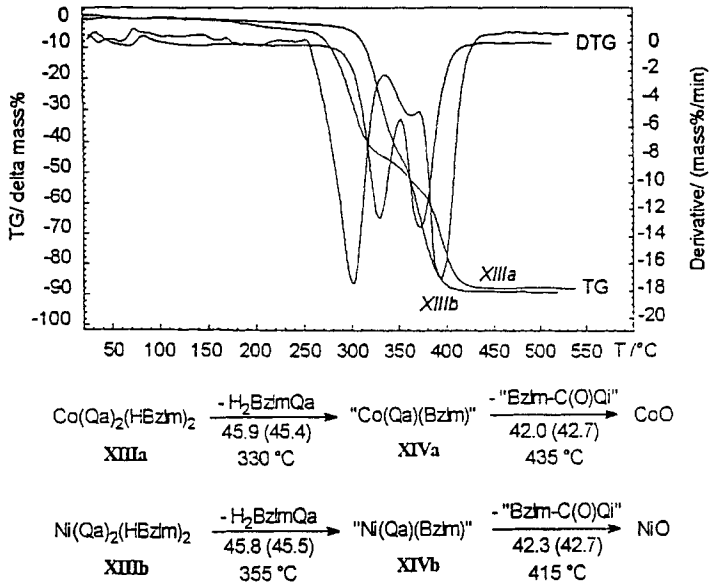

Fig. 5 Thermal degradation of $Co(Qa)_2(HBzIm)_2$ XIIIa and $Ni(Qa)_2(HBzIm)_2$ XIIIb

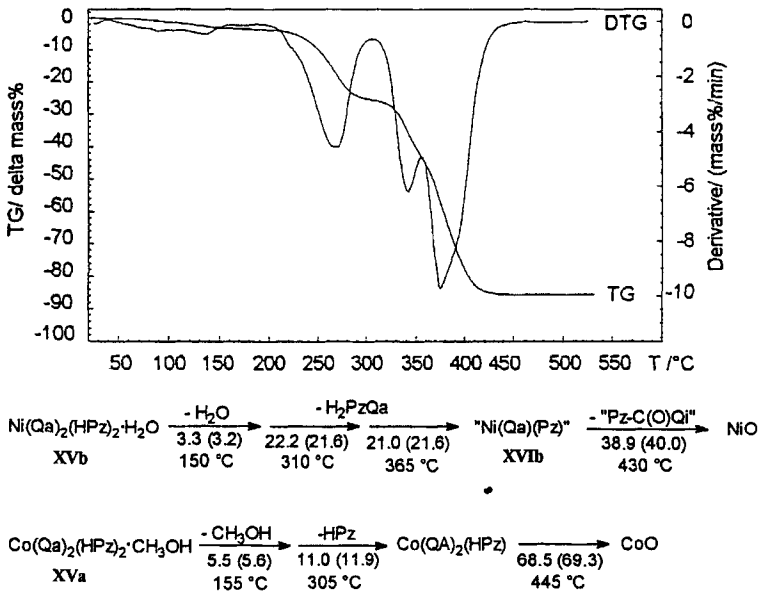

(7)

Fig. 6 Thermal degradation of $Ni(Qa)_2(HPz)_2 \cdot H_2O$ XVb

Because of the lack of the hydrogen bonds, the thermal decompositions of the complexes $M(Pa)_2(HPz)_2 \cdot 2H_2O$ XIa-b occur in a different manner. After the elimination of water, the pyrazole is released in the case of the nickel compound XIb in one step and in the case of the cobalt complex in two steps. The remaining picolinates $M(Pa)_2$ XIIa-b decompose to yield the metal oxides MO at about 400°C. Because of the formation of the complex salts $M(Pa)_2$ XIIa-b, the thermal degradation of the pyrazole adducts XIa-b is similar to that of water-containing complexes $M(Pa)_2(H_2O)_2 \cdot 2H_2O$ Ia-b.

Surprisingly, the imidazole copper complex $Cu(Pa)_2(HIm)_2 \cdot 2H_2O$ VIIc also shows a similar pattern (Fig. 4). The reason for the different thermal behaviour compared with the analogous cobalt- and nickel complexes lies in the different structure of the copper complex VIIIc. Chains of octahedrally surrounded copper units exist in the complex $Cu(Pa)_2 \cdot 2H_2O$ Ic [5]. These chains are realized by different coordinations of the picolinate oxygens one long and bridging (Cu–O=275.4(11) pm) and the other short and chelating (Cu–O=193.5(9) pm). The distorted coordination ([4+2]-octahedron) is based on the Jahn-Teller-effect [16]. Both imidazole ligands occupy the weaker coordinated apical positions in compound VIIc. For this reason, the thermal water elimination is directly followed by degradation of two moles of imidazole per mole of complex is shown in Fig. 4.

The thermal degradation of imidazole and pyrazole metal(II) quinaldinates

In the first step most of the azole adducts of the quinaldinate complexes also release azolium quinaldinate which shows an increased stability compared to free quinaldic acid. Thus, the decomposition of $Co(Qa)_2(HBzIm)_2$ XIIIa results in the formation of a blue violet tetrahedral coordinated complex, benzimidazolato-cobalt(II) quinaldinate Co(Qa)BzIm) XIVa (Fig. 5). Further thermal degradation leads to cobalt oxide, as described above. The thermolysis of $Ni(Qa)_2(HBzIm)_2$ XIIIb affords the analogous nickel product. However, the first decomposition step is shifted to higher temperature (Fig. 5). The maximum in the DTG curve which represents the thermal elimination of benzimidazolium quinaldinate, was observed at 300 and 330°C for XIIIa and XIIIb, respectively.

A tetrahedral cobalt(II) environment was detected for the coordination polymer Co(Qa)(BzIm) XIVa by determination of the magnetic moment (μ_{eff}=4.3 B.M.). On the other hand, for Ni(Qa)(BzIm) XIVb a planar $Ni(N_3O)$-coordination is assumed, which is tetragonal distorted by steric hindrance as a result of coordination polymerization [17]. In general, the change from octahedral to tetrahedral coordination occurs in the case of cobalt(II) complexes in agreement with the order of stability predicted from the spectrochemical series [18] (Fig. 5). We have reported elsewhere [7a] the same phenomena for imidazole adducts of cobalt(II) and nickel(II) acetylacetonates at lower temperature.

The further thermal behaviour of the complexes XIVa and XIVb is reversed. The latter is decomposed to NiO at 30°C lower temperature than the corresponding cobalt(II) complex. The DTG maxima differ less distinctly because of the higher decomposition temperature in contrast to the complex of the type $M(acac)_2(HIm)_2$ IIa-b with a $M(O_4N_2)$-coordination and more volatile chelating ligands [7a].

Unlike the pyrazole adducts of the metal(II) picolinates $M(Pa)_2(HPz)_2 \cdot 2H_2O$ XIa-b the corresponding quinaldinates only crystallize with one molecule of water $Ni(Qa)_2(HPz)_2 \cdot H_2O$ XVb or methanol $Co(Qa)_2(HPz)_2 \cdot CH_3OH$ XVa. The thermal degradation differs, too. Compared to the benzimidazole complex XIIIb the nickel complex XVb releases pyrazolium quinaldinate with formation of pyrazolato-nickel(II) quinaldinate Ni(Qa)(Pz) XVIb. However, there are two separate degradation steps about 100°C representing the elimination of half a mole of pyrazolium quinaldinate each (Fig. 6).

The peak splitting seems to be favoured by a multinuclear mechanism, and the pyrazolato-bridges could act as connecting link. Detected by the characteristic degradation pattern (shoulder at elevated temperature), the final decomposition to NiO takes places as mentioned above. After the removal of methanol the thermal degradation diagram of the cobalt compound XVa shows only one stage representing the release of one mol of pyrazole. According to Eq. (7) the remaining organic ligands are split off in a subsequent step.

The thermal degradation of the complexes $M(Qa)_2(HIm)_2$ XVIIa-b differs from that of other azole adducts of metal(II) picolinates and quinaldinates. In accordance with Fig. 7, the nickel compound XVIIb releases 2 moles of quinaldic acid or its decomposition products (quinoline and carbon dioxide) in separate steps in the range between 270 a 390°C.

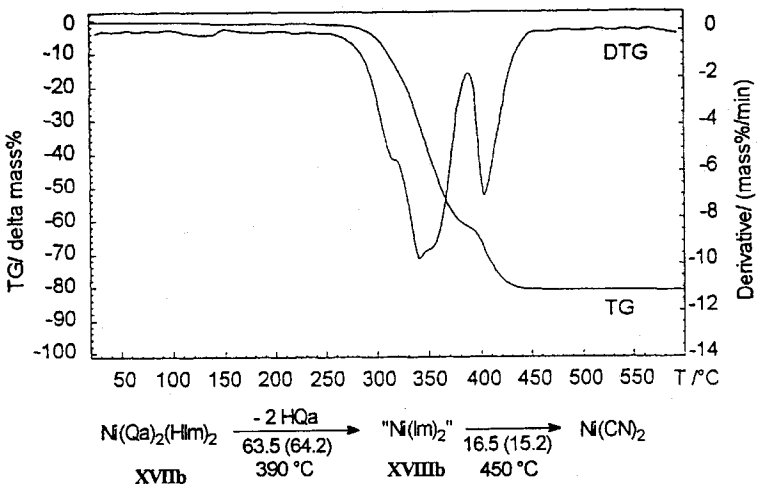

Fig. 7 Thermal degradation of $Ni(Qa)_2(HIm)_2$ XVIIb

As an intermediate, a modified $Ni(Im_2)$ XVIIIb is formed. $Ni(Im)_2$ IIIb, which can be obtained according to Eqs 1 and 2 or in direct synthesis [19], respectively, decomposes into elementary nickel below 360°C. 2,2′-Bisimidazolyl is released during this process. In accordance with Fig. 7, the high temperature modification of $Ni(Im)_2$ XVIIIb is available at about 390°C, and further heating up to 450°C causes a loss in mass of 16.5%, with $Ni(CN)_2$ as residue (about 20%). The release of the high temperature modification XVIIIb is similar to copper(I) imidazolate. Cu(Im) is also decomposed between 400 and 500°C to yield CuCN [7a, 11].

Another copper(I) compound Cu(Qa) XX is obtained by thermal degradation of imidazole or pyrazole adducts of copper(II) quinaldinates $Cu(Qa)_2(HIm)_2$ XVIIc or $Cu(Qa)_2(HPz)_2$ XVc (Fig. 8, Eq. (8)).

$$Cu(Qa)_2(HIm)_2 \xrightarrow[21.4\ (20.6)\ 240\ °C]{-HIm,\ -CO_2} Cu(Qa)(Im)(Qi) \xrightarrow[36.2\ (35.5)\ 320\ °C]{-Qi,\ -"Im"} Cu(Qa) \xrightarrow[28.1\ (30.1)\ 465\ °C]{} Cu_2O$$

XVIIc XIX XX

$$Cu(Qa)_2(HPz)_2 \xrightarrow[54.9\ (56.8)\ 315\ °C]{-"Pz",\ -HPz,\ -Qi/CO_2} Cu(Qa) \xrightarrow[28.1\ (30.1)\ 470\ °C]{} Cu_2O \qquad (8)$$

XVc XX

Fig. 8 Thermal degradation of $Cu(Qa)_2(HIm)_2$ XVIIc

The thermal process leading XX cannot be explained easily. The loss in mass in the first degradation step could be related to the elimination of imidazole and carbon dioxide. It might be due to the decarboxylation of easily decomposed chinaldic acid in the coordination sphere of copper(II). During the second thermal decomposition step the remaining quinoline (Qi) and one mole equivalent imidazolate, again as 2,2'-bisimidazolyl, is released from the copper intermediate Cu(Qa)(Im)(Qi) XIX. The reductive separation of 2,2'-bisheterocycles also allows the thermal transformation of $Cu(Im)_2$ or $Cu(Pz)_2$ into Cu(Im) or Cu(Pz), respectively [11, 17]. In the last step Cu(Qa) XX decomposes to cuprous oxide.

The crystal structure of complex $Co(Qa)_2(HBzIm)_2$ XIIIa

Suitable crystals of compound XIIIa have been obtained by recrystallizing from boiling dimethylformamide. The complex XIIIa is centrosymmetrical, while the cobalt atom has an octahedral coordination geometry and is situated at the symmetry center (Fig. 9). For this reason, the benzimidazole rings in *trans* position are twisted by 180° towards each other. This is in analogy with the corresponding complex $Co(acac)_2(HIm)_2$ IIIa [7b].

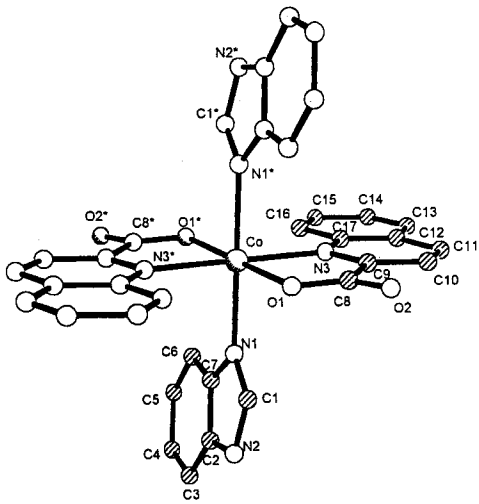

Fig. 9 Molecular structure of $Co(Qa)_2(HBzIm)_2$ XIIIa

Table 3 Selected bond distances (pm) and bond angles (deg) in $Co(Qa)_2(HBzIm)_2$ XIIIa with estimated standard deviations in parentheses

Co–O1	205.1(2)	O1–Co–N1	87.9(1)
Co–N1	217.4(3)	O1–Co–N1	77.5(1)
Co–N3	221.8(2)	N1–Co–N3	90.8(2)
O1–C8	126.0(4)	Co–O1–C8	118.5(2)
O2–C8	123.2(4)	Co–N1–C1	133.0(2)
N1–C1	139.9(4)	Co–N1–C7	121.6(2)
N1–C7	131.6(4)	Co–N3–C6	110.6(2)
N2–C2	138.1(4)	Co–N3–C17	131.4(2)
N2–C1	134.9(4)	N1–C1–N2	113.8(8)
N3–C9	132.3(4)	C1–N1–C7	104.4(3)
N3–C17	136.5(4)	O1–C8–O2	126.3(3)
C2–C7	139.6(4)	O1–C8–C9	116.3(3)
C8–C9	152.3(4)	N3–C9–C8	116.5(3)
C9–C10	139.8(5)	N3–C9–C10	123.9(3)

Table 4 Positional parameters ($\cdot 10^4$) with estimate standard deviations for XIIIa

Atom	*x*	*y*	*z*	*B*
Co	0000	0000	0000	250(1)
O1	–704(2)	–373(2)	–1400(1)	259(4)
O2	–66(3)	–558(3)	–2665(2)	468(6)
N1	–914(2)	1988(3)	–307(2)	265(5)
N2	–2505(3)	3463(3)	–1124(2)	347(6)
N3	1821(2)	614(2)	–431(2)	228(5)
C1	–903(3)	3108(3)	246(2)	273(6)
C2	–80(4)	3416(4)	1153(2)	348(8)
C3	–324(4)	4613(4)	1516(2)	431(9)
C4	–1359(5)	5502(4)	1002(3)	478(9)
C5	–2154(4)	5232(3)	114(3)	421(9)
C6	–1901(3)	4030(3)	–259(2)	303(7)
C7	–1879(3)	2264(3)	–1106(2)	321(7)
C8	147(3)	–242(3)	–1849(2)	291(7)
C9	1574(3)	365(3)	–1323(2)	263(6)
C10	2521(4)	659(4)	–1798(2)	377(8)
C11	3752(3)	1264(4)	–1329(2)	440(8)
C12	4081(3)	1544(4)	–380(2)	351(7)
C13	5345(3)	2143(5)	154(3)	52(1)
C14	5611(4)	2411(4)	1055(3)	51(1)
C15	4629(4)	2074(4)	1494(2)	390(8)
C16	3381(3)	1471(3)	1009(2)	310(7)
C17	3078(3)	1188(3)	54(2)	256(6)
H2	624	2817	1507	
H3	223	4843	2132	
H4	–1508	6314	1280	
H5	–2853	5838	–236	
HN	–3221	3843	–1633	
H7	–2113	1672	–1621	
H10	2305	440	–2436	
H11	4396	1498	–1643	
H13	6030	2363	–131	
H14	6471	2830	1398	
H15	4827	2266	2134	
H16	2721	1242	13314	

Starred atoms were refined isotropically. Anisotropically refined atoms are given in the form of the isotropic equivalent displacement parameter defined as.

$(4/3)[a^2B(1,1)+b^2B(2,2)+c^2B(3,3)+ab(\cos\gamma)B(1,2)+ac(\cos\beta)+B(1,3)+bc(\cos\alpha)B(2,3)]$

Table 5 Comparison of characteristic bond distances (pm) of selected cobalt(II) complexes

		$Co–N_{Hlm}$	Co–O	$Co–N_{acid}$	N–H···O
$Co(Qa)_2(HBzIm)_2$	XIIIa	217.4(3)	205.1(5)	221.8(2)	275
$Co(Pa)_2(H_2O)_2 \cdot 2H_2O$ [3]	Ia	–	204.5(9)	206.9(9)	–
$Co(ac)_2(Hlm)_2$ [10a]	IVa	197.4(11)	201.1(12)	–	268
$Co(acac)_2(Hlm)_2$ [7b]	IIa	215.6(3)	206.2(2)	–	297
$Co(ba)_2(Hlm)_2 \cdot 2CH_3OH$ [7b]		214.4(7)	206.0(4)	–	274

Selected bonding distances and -angles and the atom coordinates belonging to the X-ray analysis of the complex XIIIa are summarized in Tables 3 and 4. In Table 5 bonding distances around cobalt ions and hydrogen bonding distances around the imidazole nitrogen of some inner complexes are compared.

The $Co–N_{imidazole}$ and Co–O distances in XIIIa are well in the range of such bonds in similar octahedral cobalt(II) complexes. However, the $Co–N_{HBzIm}$ bond length in XIIIa is slightly (by 2–3 pm) longer than the corresponding distances in the imidazole-containing complexes. Because of the higher nitrogen-containing ligand core $[CoN_4O_2]$ the $Co–N_{acid}$ bond length in XIIIa is much more stretched (ca. 15 pm) compared to that of the aqua complex Ia. The central coordination unit in compounds Ia and IIa is $[CoN_2O_4]$. Because of the reduced coordination number in the tetrahedral cobalt(II) complex IVa, the Co–N and Co–O distances are much shorter [12a].

The weaker bonded chelating ligand in XIIIa compared to Ia should allow an easy thermal release of the free acid. Thermal elimination of quinaldic acid or benzimidazolium quinaldinate observed for XIIIa, needs to be preceded by a proton transfer from benzimidazole to the coordinated quinaldinate. Such a proton transfer is often predestined by availability of hydrogen bridges [7]. Thus,

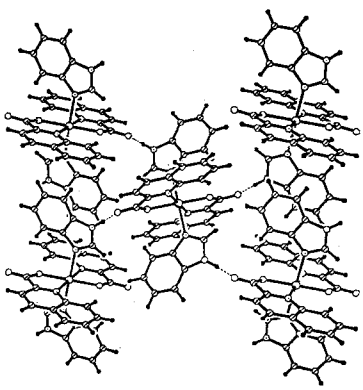

Fig. 10 Selected section of $Co(Qa)_2(HBzIm)_2$ XIIIa to illustrate the intermolecular hydrogen bridges

hydrogen bonds in complex XIIIa exist between the pyrrole nitrogen of benzimidazole and the non-coordinated oxygen of the chinaldinate ligand (Fig. 10).

The lengths and directions of hydrogen bonds are comparable to those in $Co(ac)_2(HIm)_2$ IVa (Table 3). Hydrogen bonds determine the three-dimensional structural linking of cobalt octahedrons similarly to the complex $Co(acac)_2(HIm)_2$ IIa. However, the hydrogen bridge distances of the latter compound are much longer (Table 5). A thermally initial double proton transfer in IIa is the requirement for the elimination of 2 moles of acetylacetone (Hacac) (Eq. (1)). Characteristically of azole adducts, the thermal elimination of azolium salts takes place, in other words only one proton is transferred from the azole to the heterocyclic carboxylate. Two factors act in favour of the simple proton transfer. First, the $M(N_3O)$ coordination polyhedron formed is quite stable. Secondly, the preshaped layer structure, shown in Fig. 10, is conserved. In this way, a lot of coordination compounds with nitrogen-rich coordination sphere prefer the formation of polynuclear complexes with simple imidazolate bridges against forming the homogeneous imidazolates $M(Im)_2$ [20].

The crystal structure of the benzimidazole adduct XIIIa presented here may explain the thermal release of benzimidazolium quinaldinate and the formation of the mixed ligand complex Co(Qa)(BzIm) XIVa. This thermal behaviour is dominating for the azole adducts of cobalt(II) and nickel(II) picolinates and quinaldinates. However, two different types of complexes with regard to their thermal degradation were found. One reason might be a change in the hydrogen bridge system of the complexes. This seems possible because of the small energy differences in these systems [7]. Structural determinations will be done in future. In the first degradation step the copper(II) complexes always release an azole heterocycle. This can be explained by a weaker axial coordination of the azoles caused by the Jahn-Teller-effect. In addition, the quinaldinates are thermally reduced to the copper(I) quinaldinate Cu(Qa). The azole adducts of metal(II) picolinates and quinaldinates represent latent epoxy curing agents at elevated temperature. In the above mentioned manner, the initiation of homopolymerization of epoxy resins is possible at about 150°C. Moreover, the reactivity of these compositions can be regulated by the thermal release of azolium picolinate or quinaldinate (cobalt or nickel complexes – lower activity) and pure imidazole or pyrazole (copper complexes), respectively.

* * *

We are grateful to the Fonds der Chemischen Industrie for financial support.

References

1a R. Österberg, Coord. Chem. Rev., 12 (1974) 309.
1b R. G. Bhirud and T. S. Srivastava, Inorg. Chim. Acta, 173 (1990) 121.
1c A. Dobry-Duclaux and A. May, Bull. Soc. Chim. Biol., 52 (1970) 1447.
2a K. Yamaguchi and D. T. Sawyer, Inorg. Chem., 24 (1985) 971.

2b T. Matsushita, L. Spencer and D. T. Sawyer, Inorg. Chem., 27 (1988) 1167.
2c E. Libby, R. J. Webb, W. E. Streib, K. Folting, J. C. Huffman, D. N. Hendrickson and G. Christou, Inorg. Chem., 28 (1989) 4037.
3 S. C. Chang, J. K. H. Ma, J. T. Wang and N. C. Li, J. Coord. Chem., 2 (1972) 31.
4a H. Loiseleur, G. Thomas, B. Cheverier and D. Grandjean, J. Chem. Soc. Chem. Commun., (1967) 182.
4b A. Takenaka, H. Utsumi, N. Ishihara, A. Furusaki and I. Nitta, Nippon Kagaku Zasshi, 91 (1970) 921.
5a R. D. Gillard, S. H. Laurie and F. S. Stephens, J. Chem. Soc., A (1968) 2588.
5b A. Takenaka, H. Utsumi, T. Yamamoto, A Furusaki and I. Nitta, Nippon Kagaku Zassi, 91 (1970) 928.
6 A. Böttcher, M. Döring, E. Uhlig, M. Fedtke, K. Dathe and B. Nestler, PCT-Patent 1991, WO 91/13925 from 19.09.1991.
7a M. Döring, W. Ludwig, M. Meinert and E. Uhlig, Z. anorg. allg. Chem., 595 (1991) 45.
7b M. Döring, W. Ludwig, E. Uhlig, S. Wocadlo and U. Müller, Z. anorg. allg. Chem., 611 (1992) 61.
7c W. Ludwig, M. Döring, R. Fischer, A. Friedrich, W. Seider, E. Uhlig and D. Walther, J. Thermal Anal., 42 (1994) 443.
8 M. Döring, W. Ludwig and H. Görls, J. Thermal Anal., 42 (1994) 443.
9 W. Ludwig, J. Thermal Anal., 8 (1975) 75.
10a MOLEN, An Interactive Structure Solution Procedure, Enraf-Nonius, Delft, The Netherlands 1990.
10b G. M. Sheldrick: SHELXS, Program for Crystal Structure Solution, Göttingen 1980.
11 M. Döring, Habilitation Thesis, University Jena 1994.
12a A. Gadet, Acta Crystallogr., B30 (1974) 349.
12b H. Ĺ. Henrikson, Acta Crystallogr., B33 (1977) 1947.
13 S. J. Ashcroft and C. T. Mortimer, 'Thermochemistry of Transition Metal Complexes', Academic Press, New York 1970.
14 M. Döring and H. Görls, unpublished results.
15 H. A. Staab and W. Rohr, Newer Methods of Prep. Org. Chem., 6 (1967) 61C.
16 I. B. Bersucker, Coord. Chem. Rev., 14 (1974) 357.
17 Sigwart, P. Kroneck and P. Hemmerich, Helv. Chim. Acta, 53 (1970) 177.
18 H. Irving and R. J. P. Wiliams, J. Chem. Soc. (1953) 3192.
19 R. Lehnert and F. Seel, Z. anorg. allg. Chem., 444 (1978) 91.
20 I. Bertini, L. Banci, M. Piccioli and C. Luchinat, Coord. Chem. Rev., 100 (1990) 67.